Icarus 226 (2013) 316–322

Contents lists available at SciVerse ScienceDirect

Icarus

journal homepage: www.elsevier.com/locate/icarus

Saturn's ring temperatures at equinox

Linda Spilker [a,*], Cecile Ferrari [b], Ryuji Morishima [a,c]

[a] Jet Propulsion Laboratory, California Institute of Technology, Pasadena, CA 91109, USA
[b] Laboratoire AIM Paris-Saclay, Université Paris-Diderot CEA, Irfu CNRS, INSU, F-91191 Gif-sur-Yvette, France
[c] University of California, Los Angeles, Institute of Geophysics and Planetary Physics, Los Angeles, CA 90095, USA

ARTICLE INFO

Article history:
Received 27 December 2012
Revised 16 May 2013
Accepted 1 June 2013
Available online 13 June 2013

Keywords:
Saturn, Rings
Infrared observations
Radiative transfer

ABSTRACT

Modeling the thermal emission of Saturn's rings is challenging due to the numerous heating sources as well as the structural properties of the disk and of the particles that are closely related. At equinox, however, rings are externally heated by Saturn alone and the problem is somewhat simplified. We test the abilities of our current models to reproduce the temperatures observed with the Cassini-CIRS instrument around equinox in August 2009. A simple semi-analytic model with the mutual shadowing effect can mostly explain the radial profile of the equinox ring temperatures, except the model predicts lower temperatures than those observed for the A ring. The temperature variation at a given saturnocentric radius is primarily caused by observational geometry variations relative to Saturn. The observed temperature increases with decreasing Saturn-ring-observer angle. In addition, we found evidence that the leading hemispheres of particles are warmer than the trailing hemispheres at least for the C ring and probably for the A and B rings as well. This is explained if some fraction of particles has spin rates lower than the synchronous rotation rate as predicted by *N*-body simulations. The spin model for a monolayer ring (Ferrari, C., Leyrat, C. [2006]. Astron. Astrophys. 447, 745–760) can fit the temperature variations with spacecraft longitude observed in the C ring with currently known thermal properties and a mixing of slow and fast rotators. The multilayer model (Morishima, R., Salo, H., Ohtsuki, K. [2009]. Icarus 201, 634–654) can reproduce the temperatures of the B and C rings but gives A ring temperatures that are significantly lower than those observed as does the simple semi-analytic model. More advanced models which take into account self-gravity wakes may explain the A ring temperature behavior.

1. Introduction

Modeling the thermal emission of Saturn's rings to determine their vertical structure and dynamics, as well as the ring particle physical properties is complex due to their intricate influence on the ring emitted flux. In addition, the heating of particles by multiple sources (Sun, Saturn, and nearby particles) complicates the problem. Cassini observations of seasonal effects and transient thermal regimes around the planetary shadow with varying viewing geometries may help solve parts of the puzzle.

The planet insures a constant basic heating of the rings by its infrared and visible radiation while the solar heating varies significantly as the solar elevation changes from −27° to +27° over half a saturnian year. Saturn's distance from the Sun ranges from 1.34 to 1.51×10^9 km and its orbital eccentricity is about 0.056. This also affects heating. At equinox the Sun crosses the ring plane, and its rays hit the rings at grazing incidence. During this time, the main radiation source is the infrared flux from Saturn, and the ring temperatures only weakly depend on the bolometric Bond albedo, which controls the absorbed visible flux. The temperatures of both sides of the ring disk are expected to be nearly equal because the Saturn flux is roughly the same on both sides. Heat can also be provided by nearby particles and its effect depends on ring optical depth and volume filling factor. Nearby particles are not only heating sources but also induce a screening effect between a particle and the external sources like the planet or the Sun. The equinox period is a unique period to develop a step-by-step model of the thermal emission of Saturn's rings, first by testing the ability of our current models to reproduce the ring thermal emission at this specific seasonal configuration and central heating.

In this paper, the CIRS observations of the infrared emission of Saturn's rings conducted during the equinox are presented in Section 2. In Section 3, different models currently used to analyze the data from the Cassini prime mission are compared to data. Results are discussed in Section 4.

2. Data: ring temperatures at Saturn equinox

2.1. Data analysis

CIRS consists of two Fourier transform spectrometers, which together measure thermal emission from wavelengths of 7 μm to 1 mm (1400–10 cm^{-1}) at an apodized spectral resolution

* Corresponding author.
E-mail address: Linda.J.Spilker@jpl.nasa.gov (L. Spilker).

0019-1035/$ - see front matter © 2013 Elsevier Inc. All rights reserved.
http://dx.doi.org/10.1016/j.icarus.2013.06.002

programmable from 0.5 to 15.5 cm^{-1} (Flasar et al., 2004). The far-infrared interferometer (Focal Plane 1, FP1) covers the wavelength range from 17 μm to 1 mm (600–10 cm^{-1}) and has a circular 0.25°-wide field of view. The mid-infrared interferometer consists of two 1×10 arrays of 0.2 pixels (FP3 and FP4) that together span 7–17 μm (1400–600 cm^{-1}). In this work we only use data from the long wavelength channel FP1, which includes the peak of the Planck function at Saturn's ring temperatures.

The CIRS observations which were specifically targeted to study the equinox temperatures are listed in Table 1. All consist of radial scans starting at the inner C ring boundary and ending in the outer A ring. The FP1 footprint on the rings is an ellipse whose major axis varies from hundreds to thousands of kilometers depending on spacecraft distance and elevation relative to the ring plane. Each ring region contains particles with many different spin rates, spin axis orientations, and temperatures. Their superimposed emissions produce a single spectrum. This work will concern itself with the spectral region shorter than 200 μm (longwards of the wavenumber $k = 50$ cm^{-1}), where Spilker et al. (2005) found that the emissivity, ϵ_{IR}, appears nearly constant with wavelength. A simple model for the observed intensity $I(k)$ leads to an expression in terms of the representative effective temperature, T_{eff}, and the thermal-derived filling factor, β:

$$I(k) \simeq \beta B(k, T_{eff}), \quad (1)$$

where $B(k,T_{eff})$ is the Planck function. All CIRS spectra analyzed to date resemble Planck functions so closely that the two-parameter fit works fairly well, yielding χ^2 values consistent with the Noise Equivalent Spectral Radiance (NESR) of the instrument (Spilker et al., 2005, 2006). The fit temperature T_{eff} is a representative temperature within the footprint; the parameter β is a scaling factor ranging from 0 to 1 that can be envisioned as a net emissivity of the ring structure. It is the product of the IR emissivity, ϵ_{IR}, of the individual particles surfaces, the geometrical filling factor of the ring, and the factor that arises from the temperature distribution within the field of view. For more details on the temperature retrieval, we refer the reader to Spilker et al. (2006).

2.2. Variations with saturnocentric distance a

The temperature profiles for all the radial scans are shown in Fig. 1. In the C ring, the temperature ranges between 54 K and 80 K and decreases rapidly with increasing radial distance. The dispersion between profiles at a given distance in this ring is of the order of 7–8 K. In the B ring, the radial trend is similar and the temperature varies on average between 58 K and 45 K. The dispersion among B ring profiles is less than in the C ring, only about 3–4 K. The Cassini Division (CD) is often not resolved and the data are very noisy. The temperature range here is similar to that for the B ring despite a larger distance to Saturn. This is most likely due to its low optical depth and therefore smaller shadow-hiding between particles which allows more of Saturn's radiation to be absorbed. The A ring temperatures are almost identical to those for the outer B ring. Overall, the radial temperature variations for the A and B rings are smaller than those for the C ring.

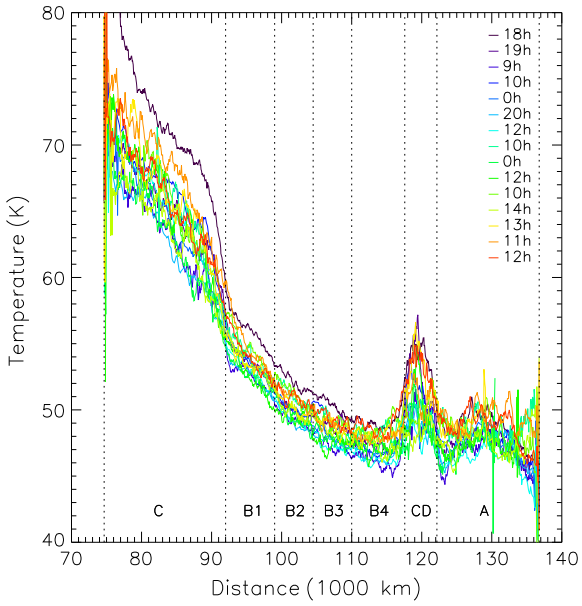

Fig. 1. Ring temperature versus saturnocentric distance as measured by the CIRS spectrometer at equinox (Table 1). The profiles are color coded from black to red with time elapsed since the equinox date. The local hour angles (L) of the radial scans are also shown in units of hours (1 h = 15°). For each location, the standard deviation is calculated using nearby temperatures (±1000 km). After removing temperatures outside 3-σ, smoothing is applied using the nearby 10 temperatures. The temperature and the optical depth are anticorrelated and the temperature decreases with distance, as expected for the case of central heating. (For interpretation of the references to color in this figure legend, the reader is referred to the web version of this article.)

These observations took place when the solar elevation was between 0° and 0.036° above the ring plane, mostly after the equinox. Due to these very low elevations, the expected input solar flux $F_{\odot}\sin|B'|$ to the ring plane, where $F_{\odot} = 15.6$ W m^{-2} is the solar flux at Saturn's distance and B' is the solar elevation angle, is negligible as compared with the infrared flux from Saturn. The infrared flux from Saturn received by a ring particle without shadowing from other particles is given by

$$F_S = I_{S,IR}\Omega_S, \quad (2)$$

where $I_{S,IR} = \sigma_{SB}T_S^4/\pi$ is the thermal intensity emitted from Saturn, σ_{SB} is the Stefan–Boltzmann constant, T_S is the effective temperature of Saturn, $\Omega_S = 2\pi\left(1 - \sqrt{1 - (R_S/a)^2}\right)$ is the solid angle of Saturn seen from the ring (Saturn's oblateness is ignored here but taken into account in models in Section 3), R_S is Saturn radius. The expected particle temperature is given by

$$T = \left(\frac{F_S}{f\sigma}\right)^{1/4}, \quad (3)$$

Table 1
CIRS observations. All data were obtained in 2009.

Obs. Name: CIRS_116RI_*	Date start	Date end	B' (°)	$B^a_{S/C}$ (°)	α^a (°)	L (h)	$L^a_{S/C}$ (h)
EQLBS001_PRIME	223T01:35:00	223T06:35:00	−0.00007	15.7	147	18, 19	1
URALPVIR002_UVIS	223T14:00:13	223T16:58:53	0.009	17	30	9	13
EQSBS001_PRIME	224T03:00:00	224T06:00:00	0.017	21	64	0, 20, 12, 10	16
EQLBN001_PRIME	225T02:16:53	225T08:11:43	0.03	19	86	10, 0, 12	17.7
TMAPN20MP001_PRIME	225T09:12:23	225T14:45:53	0.036	18	93	10, 14, 13, 11, 12	17.9

[a]: On average. B': solar elevation angle, $B_{S/C}$: spacecraft elevation angle, α: phase angle, L: local hour angle around Saturn for the radial scan, $L_{S/C}$: spacecraft local hour angle around the footprint. L and $L_{S/C}$ are in units of hours (1 h = 15°). The Sun–Saturn distance is $D_{UA} = 9.43$ UA at epoch.